

Crystalline layer in *Drosophila melanogaster* eggshell: arrangement of components as revealed by negative staining and reconstruction

S. J. Hamodrakas and L. H. Margaritis

Department of Biology, University of Athens, Panepistimiopolis, Kouponia, Athens (621), Greece

and P. E. Nixon*

Asbury Department of Biophysics, University of Leeds, Leeds LS2 9JT, UK

(Received 6 April 1981; revised 10 June 1981)

*Eggshell formation in *Drosophila melanogaster* is used as a model system in studies of cellular differentiation. A detailed knowledge of eggshell structure is necessary for this purpose and also to permit correlation of eggshell structure with function. Unique among the eggshell layers, the innermost chorionic layer (ICL) was investigated by means of transmission electron microscopy of thin sections and whole mounts, utilizing conventional fixation, LaNO_3 impregnation and negative staining with uranyl acetate. Whole mount face views of negatively stained ICLs were processed by means of optical and computer reconstruction. The ICL, which almost fully covers the oocyte, consists of 4–5 bilaminar sublayers with a total thickness of 400–500 Å. It appears to be formed by crystallites, 1–2 µm in size, containing roughly spherical molecules which are 30 Å in diameter approximately. Each unit cell probably includes 8 molecules and also distinct vacant spaces, differing in size. ICL may be involved in the exchange of the respiratory gases during embryogenesis.*

Keywords: Thin sections (microscopy); chorion; eggshell; *Drosophila*; crystalline; reconstruction

Introduction

The eggshell of *Drosophila melanogaster* is formed by the follicular epithelium, according to a temporal developmental program of specific protein synthesis¹, and consists of several distinct layers^{2,3} (vitelline membrane, wax layer, innermost chorionic layer, endochorion and exochorion). Unique among them, the innermost chorionic layer (ICL, formerly 'intermediate chorionic layer'⁴) which lies between the wax layer and the endochorion, exhibits a crystalline structure in the mature egg^{3,4}. Similar crystalline layers have been reported to occur in several orders of insects⁵. One possible function of the ICL is to facilitate formation of the wax layer, by pressing it against the vitelline membrane (Margaritis, unpublished results). The ICL, together with the endochorion, shows peroxidase activity⁶. Moreover, electron microscopical studies have revealed that the ICL gross structural features are very similar in various *Drosophila* species (Margaritis, unpublished observations), whereas a number of alterations, sometimes major, have been observed in the structure of other eggshell constituents (mainly in the endochorion and the respiratory appendages).

Analysis of the innermost chorionic layer is part of our efforts to investigate in detail the structure and composition of the *Drosophila melanogaster* eggshell, in order to understand the relationship between structure and function of the various eggshell constituents, the mechanisms of eggshell formation and the mechanisms of action of eggshell mutations.

In this study we present data revealing the arrangement of the ICL component molecules in projection and we propose a possible model for its 3D organization.

Experimental

Specimen preparation and electron microscopy

(1) Flat sheets of ICL, together with vitelline membrane, were isolated from laid eggshells⁴, mounted on copper grids and negatively stained with 2% uranyl acetate. Some samples were washed with distilled water after staining and prior to drying.

(2) Late stage 14 follicles¹ were fixed with glutaraldehyde in the presence of 1% lanthanum nitrate⁷ and processed for electron microscopy as described elsewhere³.

(3) Electron microscopy was performed using Phillips EM200 and EM301 microscopes. The latter was equipped with a goniometer stage.

Image processing

(a) Optical diffraction and filtering were performed using a He-Ne laser diffractometer, as described previously⁴.

(b) Computer reconstruction:

Method A. Micrographs were measured on a scanning digital microdensitometer (Optronics P1000, SRC Daresbury Laboratory, Daresbury, England). The optical density measurements from selected areas were processed on the Leeds University ICL 1906A computer. An area of measurements, typically 120 × 120 was put into an array 200 × 200, the remaining array elements being set equal to

* Present Address: Westcott House, Jesus Lane, Cambridge CB5 8BP, UK.

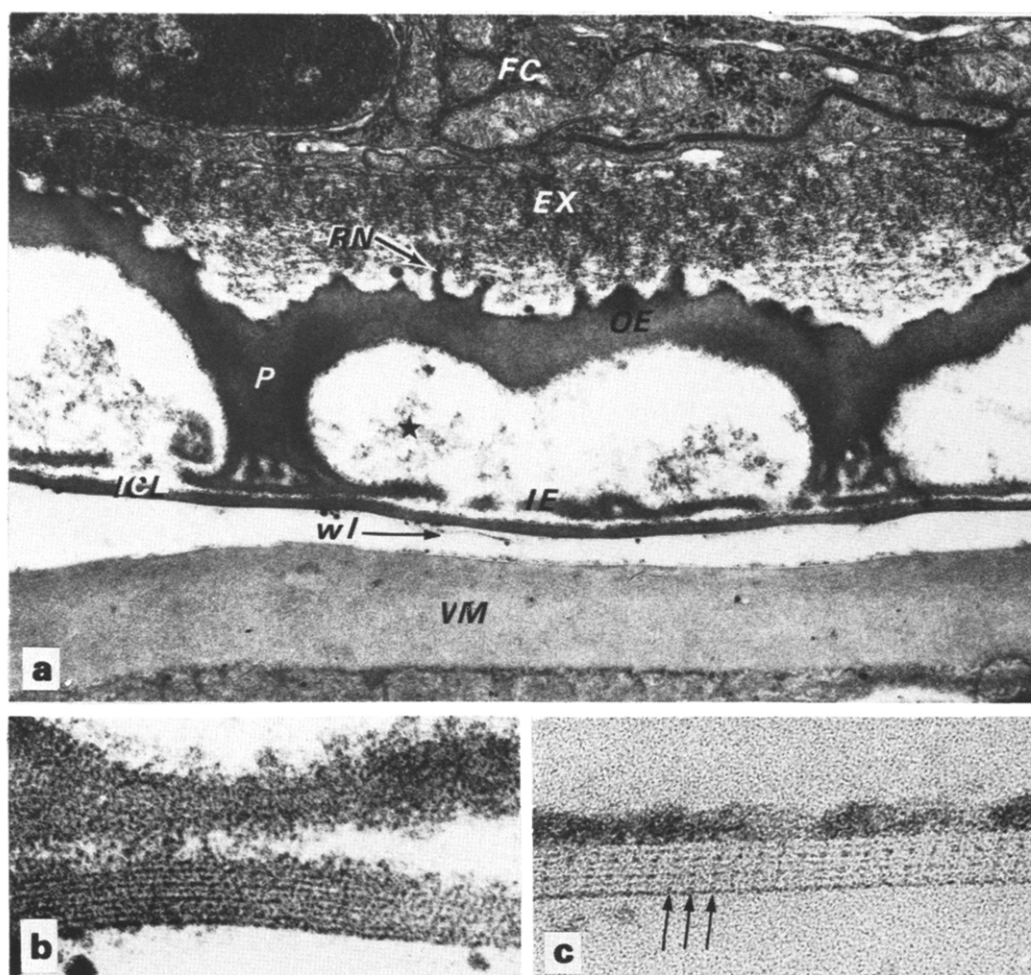


Figure 1 (a) A thin sectioned mature *Drosophila melanogaster* follicle showing part of the oocyte, the vitelline membrane (VM), remnants of the wax layer (wl), the innermost chorionic layer (ICL), the endochorion, which consists of floor (IE), pillars (P), roof (OE), and roof network (RN), the fibrous exochorion (EX) and the degenerating follicle cells (FC). Magnification $\times 35\,000$. (b) Higher magnification image of a thin sectioned mature follicle. The innermost chorionic layer, 400–500 Å in thickness, is seen to consist of 4–5 bilaminar sublayers. Magnification $\times 200\,000$. (c) Innermost chorionic layer from a thin sectioned mature follicle after impregnation with LaNO_3 . The stain has been absorbed at the outer surface of the layer but has also entered within the sublayers revealing a quasi-tetragonal arrangement (arrows). Magnification $\times 150\,000$

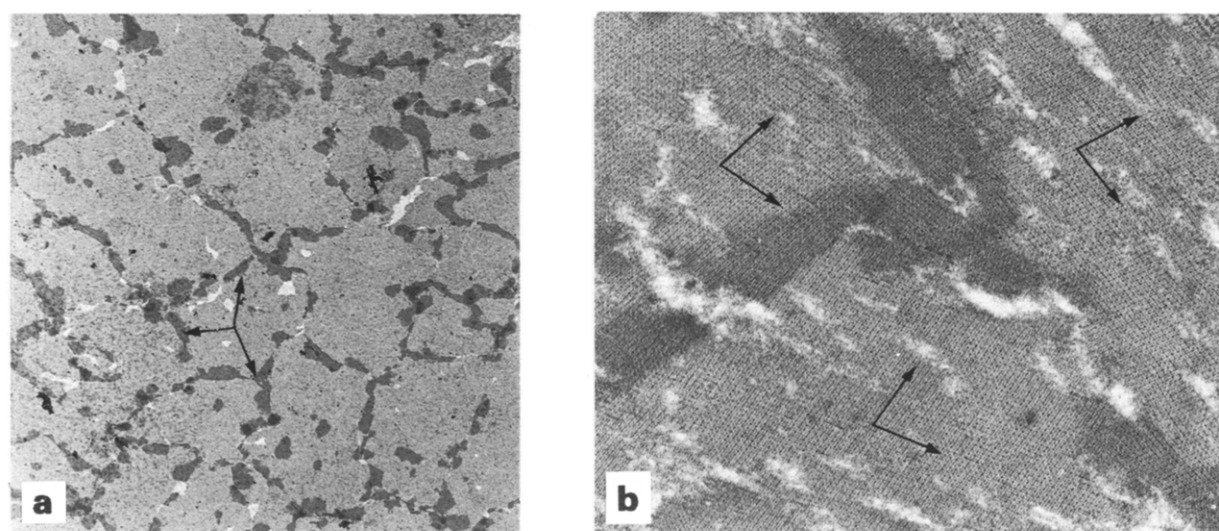


Figure 2 (a) Whole mount face view of a negatively stained (with uranyl acetate) innermost chorionic layer. Under low power the layer is seen to consist of irregularly shaped crystallites 1–2 μm in size (arrows). Magnification $\times 7500$. (b) Adjacent crystallites reveal, usually, different orientations in the directions of the periodic accumulation of stain (angled arrows). Magnification $\times 70\,000$

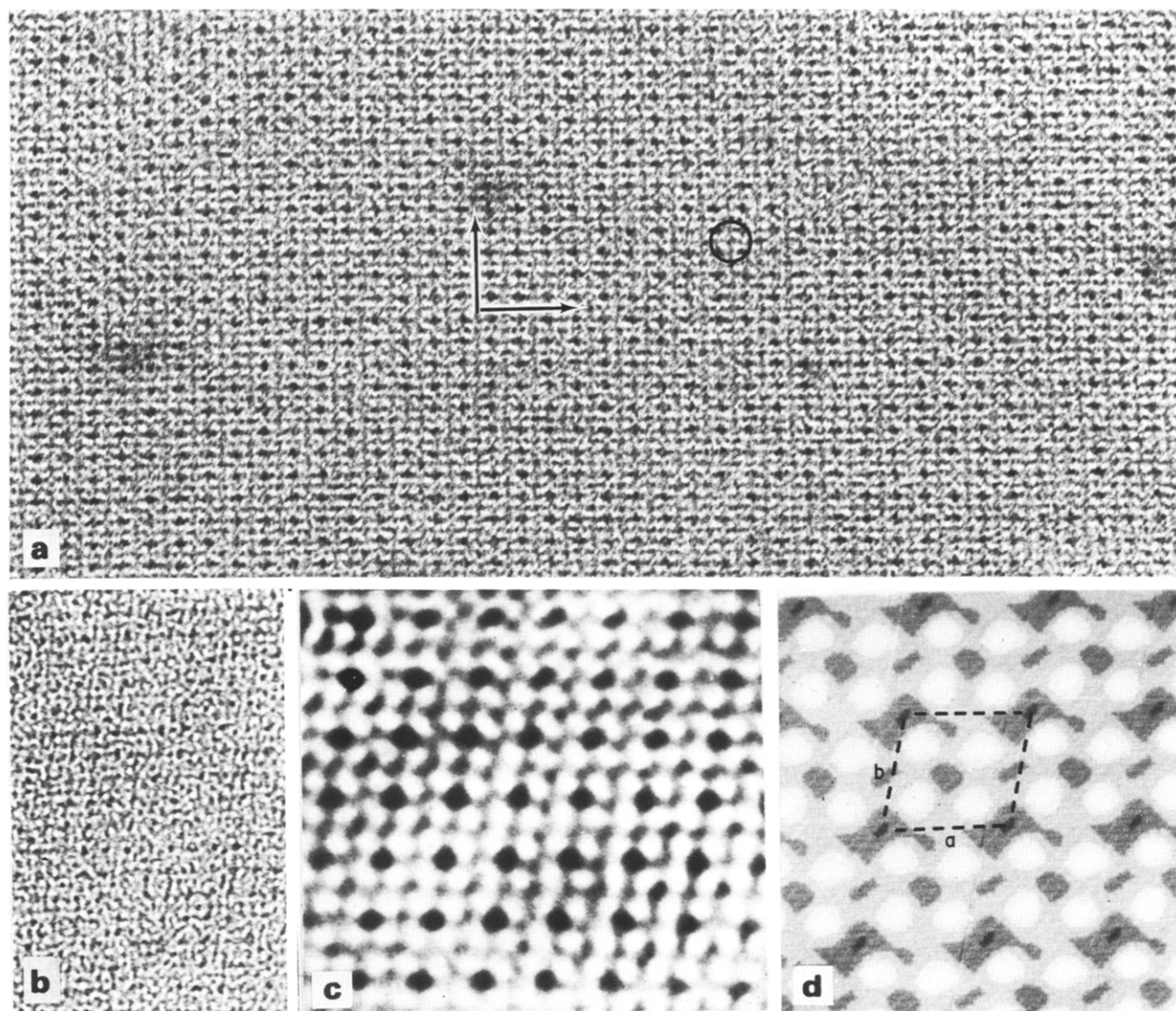


Figure 3 (a) High magnification whole mount face view of a negatively stained ICL, revealing the arrangement of electron dense spots, and of white, electron transparent, domains in tetrads (circle), which represent in projection through the sublayers, the actual (protein?) components of the layer. Faint striations (arrows) are seen also to exist between the electron dense spots. Magnification $\times 440\,000$. (b) Electron micrograph of an isolated ICL, negatively stained with uranyl acetate, used for optical (*Figure 3c*) and computer (*Figure 3d*) reconstructions. The variation of the unit cell parameters (see text) is obvious by comparison with *Figure 3a*. Magnification $\times 440\,000$. (c) Optically filtered image of the ICL shown in *Figure 3b*. Magnification $\times 1\,100\,000$. (d) Computer reconstructed image of the ICL shown in *Figure 3b* (method A), which reveals major and minor electron dense spots, as well as electron transparent (white) domains, representing in projection the actual molecules of the layer. The unit cell is outlined by broken lines. Twelve shades of grey were used to give a shaded appearance. Magnification $\times 2\,070\,000$

the mean value of the measurements⁷. The Fourier transform of the enlarged array was performed using an algorithm of the Cooley-Tukey type and took about 13 s. The reciprocal lattice was clearly visible in the Fourier transform and the structure factors were found by fitting the real and imaginary parts of the transform to the expected peak shape by a least squares procedure. The shape of the peaks should be the Fourier transform of the shape of the 120×120 region in the data arrays: in our case a two dimensional sinc function⁸; all but the very weakest structure factors fitted this shape. The lattice parameters were refined by maximizing the sum of the structure factor intensities, and a suitable region of the original micrographs was chosen, on the basis of a high sum of intensities and of strong high order spots. The reconstruction was performed on the PDP 11/45 computer in the Department of Biophysics at Leeds University. The structure factors were used to calculate

the stain density in one unit cell, on a 40×40 grid. Several adjacent cells were displayed on the interactive graphics screen as dots of varying brightness and photographed. The dots were moved during the exposure (~ 30 s) to give a shaded appearance.

Method B. Reconstructions of another set of electron micrographs were performed, utilizing a fully automated system developed at the Rosenstiel Basic Medical Sciences Research Center, Brandeis University, Waltham, Mass. USA (D. J. DeRosier, unpublished results). This system uses an Optronics P1000 scanner, a PDP 11/40 computer and a Grinnel Graphics Television Imaging System (GMR-27). The set of programs controlling the system (OPFSMT, EMBOX, EMFOUR, EMDSP, EMMASK, EMFILT) has been constructed according to the theory given by D. J. DeRosier and P. B. Moore⁹.

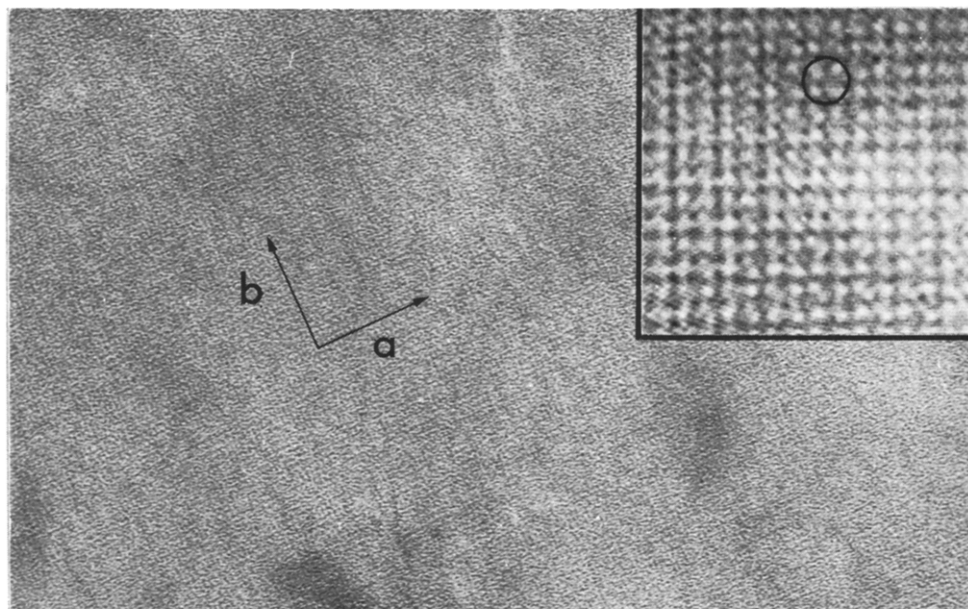


Figure 4 Isolated ICL, negatively stained with 2% uranyl acetate and washed in distilled water before air-drying. Fine striations with a 50 Å pseudoperiodicity are emerging in two directions (axes a and b). The inset is an optically filtered image of this micrograph showing the arrangement of the electron transparent domains (circle). Magnification $\times 125\,000$, inset $\times 500\,000$

Results and discussion

A thin sectioned mature (late stage 14) follicle, after a conventional fixation-staining procedure (glutaraldehyde followed by osmium tetroxide), reveals clearly most eggshell layers: vitelline membrane (VM), innermost chorionic layer (ICL), inner endochorion (IE), pillars (P), outer endochorion (OE), roof network (RN), exochorion (EX) and vaguely the wax layer (wl) (Figure 1a). Viewed under higher magnification, the ICL is shown to consist of 4–5 bilaminar sublayers, with a total thickness of about 400–500 Å (Figure 1b). After impregnation with lanthanum nitrate during fixation, with no other staining, large deposits of stain are seen to exhibit a periodicity of ~ 100 Å in two directions: one perpendicular and the other parallel to the sublayers (Figure 1c). Therefore, it would seem that, there are regularly spaced vacant areas within the ICL, the colloidal lanthanum micelles can enter and precipitate during dehydration.

Whole mount face views of the layer, after isolation and negative staining⁴, reveal under low power that the ICL consists of numerous crystallites $1\text{--}2\ \mu\text{m}$ in size (Figure 2a). In each crystallite electron dense deposits of stain are seen to form a two dimensional lattice (Figure 2b). Adjacent crystallites differ from one another in the direction of their lattice vectors. Apparently, this is an inherent property of the ICL and not a consequence of the isolation procedure or specimen preparation: most probably it is related to the process of the ICL formation: There are indications (Margaritis, unpublished observations) that the ICL crystallites are formed by a self-assembly procedure, from a number of separate nucleation centres during choriogenesis; these nucleation centres may correspond to the endochorionic pillars which have a similar distribution.

Under higher magnification, it is clear that the arrangement of the electron dense deposits of stain in these whole mount face views of the layer (Figure 3a) is almost identical to the cross-sectioned views (compare with Figure 1c). Each tetrad of major electron dense spots

surrounds a set of four electron transparent domains (Figure 3a, circle) which presumably represent, in projection, spaces occupied by actual ICL molecules. Furthermore, minor electron dense spots or striations are found between the major, 100 Å spaced, electron dense spots.

Different ICLs or different areas of the same ICL examined by negative staining in whole mount, show variations in the unit cell parameters of the two dimensional lattice (Figures 3a and 3b). The unit cell axial lengths vary between 75 and 100 Å and the interaxial angle is in the range 75–90°; the values of the cell parameters appear to be uniformly distributed in these ranges. There are several possible reasons for these variations, the most obvious being distortions produced during the air-drying procedure and differences of orientation of the ICL sheets with respect to the electron beam.

Further analysis with optical diffraction and filtering and also computer reconstruction (method A) of electron micrographs (Figures 3c, 3d correspondingly) confirmed the structural features indicated by the initial micrographs. In each unit cell (Figure 3d), four electron transparent domains of nearly circular shape, ~ 30 Å in diameter, are seen to be related by an approximate fourfold rotation axis and represent in projection the structural elements of the ICL; these are probably protein molecules, since it is almost certain that protein is the main constituent of this chorionic layer⁵. Dimensions of the order of 30 Å are not unexpected for protein molecules¹⁰.

Negatively stained ICLs, washed before drying, do not show periodicities arising from dense accumulation of stain every 100 Å, but, instead, less dense striations, spaced every 50 Å approximately (Figure 4). Therefore, it would seem that washing the specimen prior to drying results in staining the ICL to a lesser extent as a whole, hence the reduced overall contrast seen in Figure 4. Nevertheless, we believe that this procedure removes a

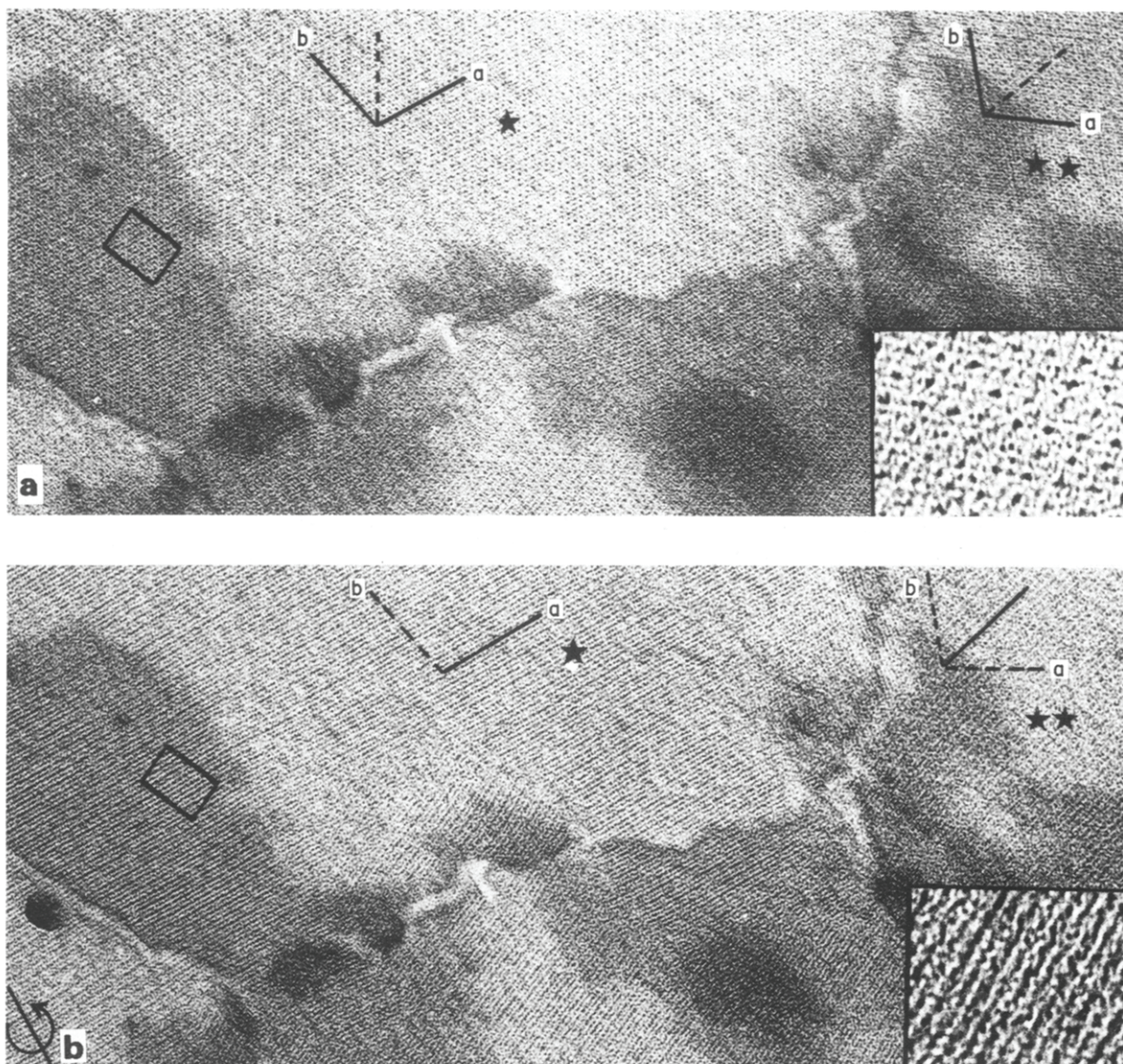


Figure 5 (a) and (b) Representative micrographs from a tilt series of a negatively stained, isolated, ICL at $+6^\circ$ and -18° respectively. Observe the periodic distribution of stain at the two crystallographic axes *a* and *b*, in two adjacent crystallites (one and two asterisks) in *Figure 5a*. Striations are seen to exist in a direction almost bisecting the angle of the two axes (broken lines). In *Figure 5b*, overlapping electron dense spots can be seen along the *a*-axis of one crystallite (one asterisk) and no periodicities along the *b*-axis, whereas in the other crystallite (two asterisks) there is no trace of electron dense spots along the axes *a* and *b*, but, just white striations in a direction bisecting the interaxial angle (solid line, compare with broken line in *Figure 5a* — two asterisks). The tilt axis, shown at the lower left, is almost perpendicular to the *a*-axis of the crystallite marked with one asterisk. Magnification $\times 125\,000$, insets $\times 450\,000$

large part of the stain from the 'wide' vacant spaces of the ICL, having a periodicity of 100 Å, but to a minor part from the 'narrow' ones which intervene, thus resulting in a 50 Å pseudoperiodicity. Optical reconstruction of this sample (*Figure 4*, inset) confirms the existence of the electron transparent domains forming tetramers, which are repeated every 100 Å in two crystallographic directions.

It remained to be clarified whether the observed two dimensional periodicity on the whole mount face views of the ICL arises from adsorption of stain on the surface of the ICL, or whether the stain (uranyl acetate) is distributed internally within the layer, as is lanthanum nitrate (*Figure 1c*). To answer this question, an isolated, negatively stained ICL was observed at various angles of tilt with respect to the electron beam. Micrographs of the same area of the ICL were obtained at intervals of 6° , from -18° to $+18^\circ$. In *Figure 5a* ($+6^\circ$ tilt) the boundaries of 4

crystallites, of those forming the polycrystalline structure of the ICL, can be seen clearly. The direction of the axis of tilt was chosen almost perpendicular to the *a* axis of the crystallite marked with one asterisk. This micrograph shows the two dimensional periodicity of the electron dense spots most clearly, and thus is considered to represent a nearly perpendicular orientation of the layer with respect to the electron beam. At a tilt angle of -18° , in the same crystallite (*Figure 5b*, one asterisk and inset), multiple electron dense spots appear along a crystallographic direction (*a*-axis) perpendicular to the axis of tilt, while striations along the *b*-axis are no longer visible. In an adjacent crystallite with different orientation (*Figure 5b*, two asterisks), the periodicity of the electron dense spots disappears, while light striations are emerging along a direction almost bisecting the angle of the crystallographic axes.

The patterns obtained by optical diffraction analysis of

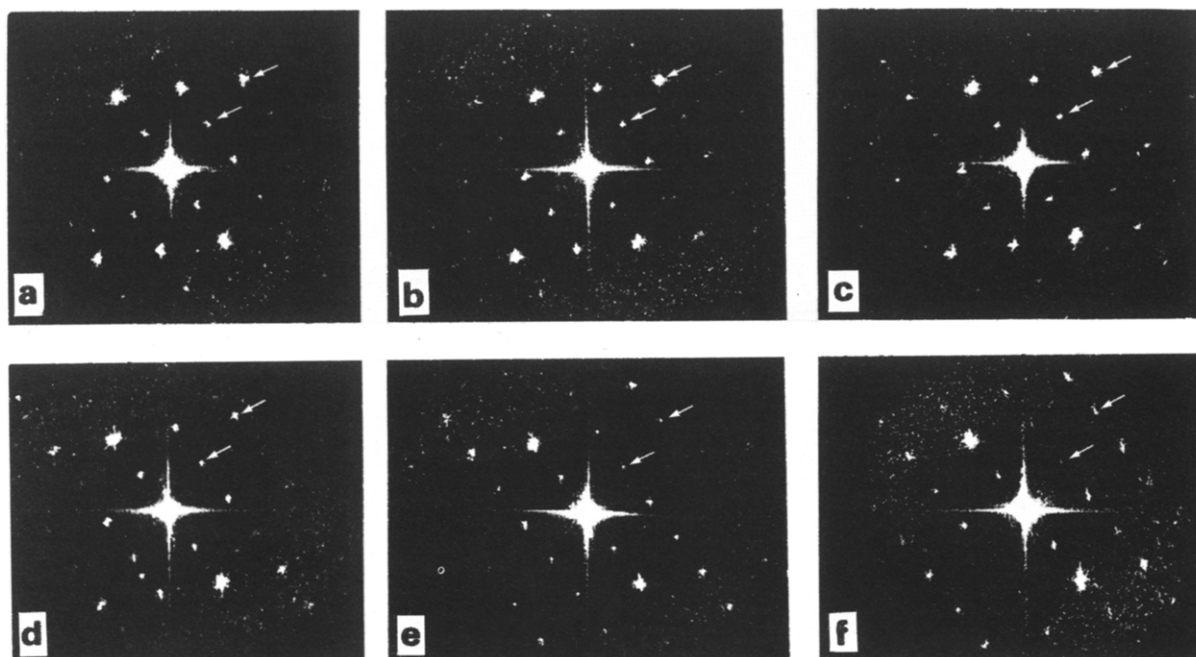


Figure 6 (a), (b), (c), (d), (e) and (f) Optical diffraction patterns from the same area (solid box in the crystallite marked with one asterisk in *Figure 5a*) of the micrographs obtained at $+18^\circ$, $+12^\circ$, $+6^\circ$, 0° , -6° , -12° angles of tilt correspondingly. A gradual decrease is observed in the intensity of the 1st and 2nd order spots, which correspond to periodicities perpendicular to the tilt axis

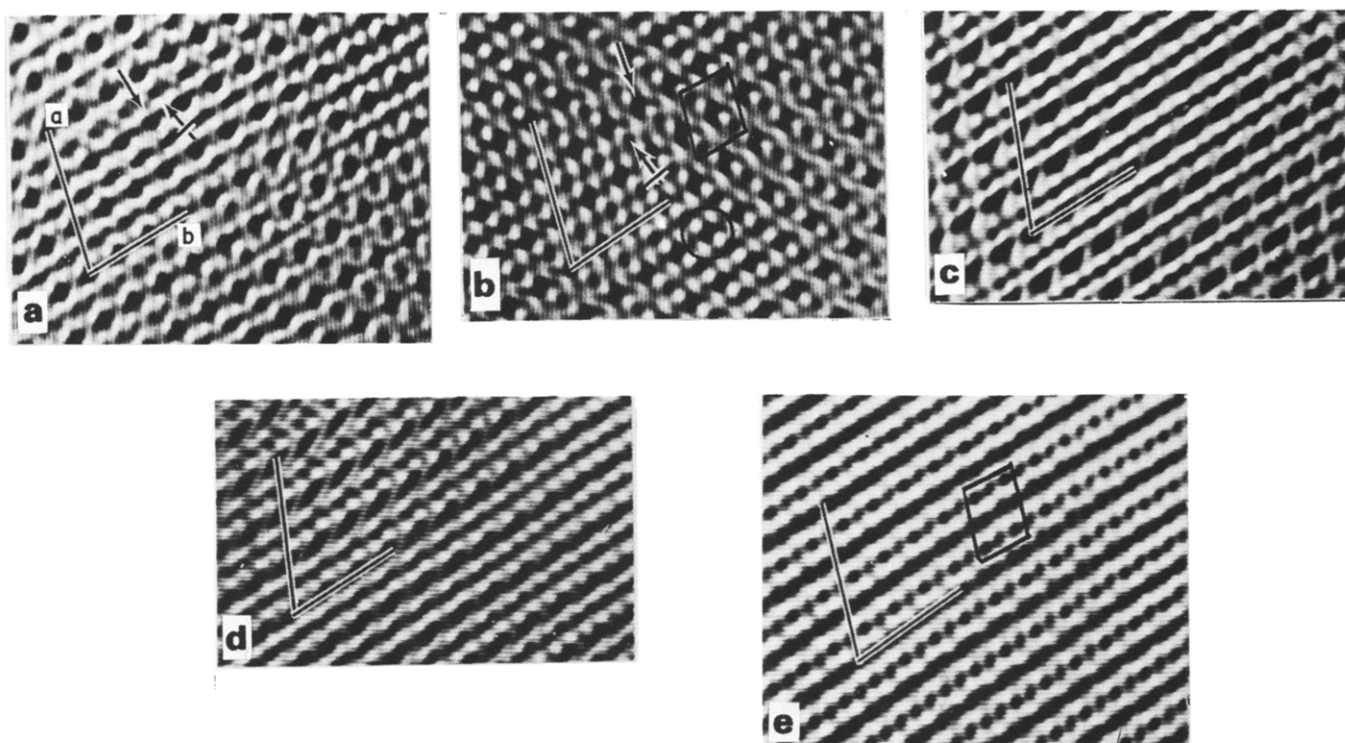


Figure 7 Computer reconstructed images of micrographs obtained at various angles of tilt, from an isolated, negatively stained, ICL (method B). (a) $+18^\circ$ tilt: major electron dense spots (arrow) are repeated along two axes, a and b. Minor spots (crossed arrow) are located off-centre in respect to the major spots (compare with $+6^\circ$ tilt). (b) $+6^\circ$ tilt: major spots (arrow) form a basic repeating unit, including a minor spot at the centre (crossed arrow). Observe the transparent domains (circle), representing in projection the 'biomolecules, surrounding each major (and also minor) spot. Minor spots are very clearly resolved (solid box). (c) 0° tilt: major and minor electron dense spots are elongated along the a-axis which is perpendicular to the tilt axis. (d) -6° tilt: similar arrangement as in 0° tilt. (e) -18° tilt: all spots are seen double compared to the $+6^\circ$ tilt (compare solid boxes), an indication that the image is a projection of the internal structure of the layer, as outlined by negative staining through the sublayers. Magnification $\times 650\,000$

the same area (Figure 5a, parallelogram) under various angles of tilt (Figure 6) reveal a gradual decrease in the intensity of the first and second order spots (Figure 6, arrows), in a direction perpendicular to the axis of tilt.

Computer reconstructions of the images obtained at $+18^\circ$, $+6^\circ$, 0° , -6° and -18° were performed employing a fully automated system (method B). The reconstructions (Figure 7) showed that, as the specimen was tilted about an axis perpendicular to the *a*-axis, both major and minor electron dense spots were first elongated and then resolved into double spots.

These observations indicate that the image we obtain (e.g. Figure 3a) is due not simply to adsorption of negative stain on the surface of the ICL, but arises from penetration of the stain into its sublayers.

Combining the information provided by the reconstructions of the whole mount face views of the ICL (Figures 3c, 3d and 7) with the appearance of its cross sections (Figure 1c), we suggest that an octameric arrangement of probably spherical protein molecules is a plausible basic repeating unit in the crystalline structure of the ICL. Nevertheless, this is not certain and awaits further experimental evidence.

It would appear that the spaces occupied by the negative stain (Figures 1c, 3c and 3d) are wide enough *in vivo* to allow exchange of the respiratory gases to occur freely through the ICL during embryogenesis.

In conclusion, the results reported in this study demonstrate the crystallinity of the ICL. Information obtained from various projections of the ICL suggests that its constituent (protein ?) molecules are roughly spherical in shape, with dimensions of the order of 30 Å; their packing arrangement leaves intervening spaces which may be of physiological importance.

Experiments are in progress to investigate the three dimensional structure of the ICL further, by 3D reconstruction and by techniques such as low-dose electron diffraction¹¹; other experiments are directed

towards analysis of the morphogenesis of this interesting structure.

Acknowledgements

We are very grateful to Prof. D. J. DeRosier for his help, for use of his optical diffractometer and for making available to us his automated system and to Profs. F. C. Kafatos and A. C. T. North for useful comments. We would also like to thank the SRC Densitometer Service at the SRC Laboratory, Daresbury, England for the use of their densitometer and the Leeds University Computing Laboratory for the provision of computing facilities.

This investigation was supported by grants awarded to S.J.H. by Athens University and to L.J.M. by NATO (No. 1397), by Athens University and by the A. Onassis foundation. Travelling expenses to the USA, for S. J. H. were provided by the Greek Ministry of Coordination.

References

- 1 Petri, W. H., Wyman, A. R. and Kafatos, F. C. *Dev. Biol.* 1976, **49**, 185
- 2 Margaritis, L. H. *Ph. D. Thesis*, University of Athens (1974)
- 3 Margaritis, L. H., Petri, W. H. and Kafatos, F. C. *J. Cell Sci.* 1980, **43**, 1
- 4 Margaritis, L. H., Petri, W. H. and Wyman, A. R. *Cell Biol. Int. Rep.* 1979, **3**, No. 1, 61
- 5 Fourneaux, P. J. S. and Mackay, A. L. *J. Ultrastruct. Res.* 1972, **38**, 343
- 6 Mindrinos, M. N., Petri, W. H., Galanopoulos, V. K., Lombard, M. F. and Margaritis, L. H. *Roux Archives Dev. Biol.* 1980, **189**, 187
- 7 Revel, J. P. and Karnovsky, M. J. *Cell Biol.* 1967, **33**, C7-C12
- 8 Lee, D. L., Nixon, P. E. and North, A. C. T. *Proc. R. Soc. London (B)* 1980, **208**, 409
- 9 Derosier, D. J. and Moore, P. B. *J. Mol. Biol.* 1970, **52**, 355
- 10 Schulz, G. E. and Schirmer, R. H. in 'Principles of Protein Structure', Springer-Verlag, New York-Heidelberg-Berlin, 1978
- 11 Unwin, P. N. T. and Henderson, R. *J. Mol. Biol.* 1975, **94**, 425